Biosensors and Bioelectronics 137 (2019) 117–122

Contents lists available at ScienceDirect

Biosensors and Bioelectronics

journal homepage: www.elsevier.com/locate/bios

Remarkably enhanced photoelectrical efficiency of bacteriorhodopsin in quantum dot – Purple membrane complexes under two-photon excitation

Victor Krivenkov[a,*], Pavel Samokhvalov[a], Igor Nabiev[a,b,**]

[a] Laboratory of Nano-Bioengineering, National Research Nuclear University MEPhI (Moscow Engineering Physics Institute), 115409, Moscow, Russian Federation
[b] Laboratoire de Recherche en Nanosciences, LRN-EA4682, Université de Reims Champagne-Ardenne, 51100, Reims, France

ARTICLE INFO

Keywords:
Quantum dots
Membrane protein
Bacteriorhodopsin
Two-photon excitation
Resonance energy transfer
Photoelectrochemistry

ABSTRACT

The photosensitive protein bacteriorhodopsin (bR) has been shown to be a promising material for optoelectronic applications, but it cannot effectively absorb and utilize light energy in the near-infrared (NIR) region of the optical spectrum. Semiconductor quantum dots (QDs) have two-photon absorption cross-sections two orders of magnitude larger than those of bR and can effectively transfer the up-converted energy of two NIR photons to bR via the Förster resonance energy transfer (FRET). In this study, we have engineered a photoelectrochemical cell based on a hybrid material consisting of QDs and bR-containing purple membranes (PMs) of *Halobacterium salinarum* and demonstrated that this cell can generate an electrical signal under the two-photon laser excitation. We have shown that the efficiency of light conversion by the PM–QD hybrid material under two-photon excitation is up to 4.3 times higher than the efficiency of conversion by PMs alone. The QD integration into the bR-containing PMs significantly improves the bR capacity for utilizing light upon two-photon laser excitation, thus paving the way to the engineering of biologically inspired hybrid NIR nonlinear optoelectronic elements. The nonlinear nature of two-photon excitation may provide considerable advantages, such as a sharp sensitivity threshold and the possibility of precise three-dimensional location of excitation in holography and optical computing.

1. Introduction

Bacteriorhodopsin (bR) is a unique ultrastable protein with photochromic properties capable of converting the energy of light into chemical and electrical energies (Oesterhelt and Stoeckenius, 1971). In its natural form, bR is the only transmembrane protein of the purple membranes (PMs) of the bacteria *Halobacterium salinarum* (Oesterhelt and Stoeckenius, 1971; Hampp, 2000). Geometrically, a PM is a two-dimensional hexagonal lattice with a period of about 6.2 nm (Butt et al., 1990; Rakovich et al., 2010; Bouchonville et al., 2011), in whose nodes trimers of bR molecules are located. The typical thickness of these membranes is 5.25–5.70 nm, and the distance between bR molecules in the trimers is about 3.5 nm. Under the excitation by light in the visible region of the optical spectrum, the photosensitive unit of bR, retinal (a derivative of vitamin A), undergoes reversible isomerization from the all-trans form to the 13-cis one through a series of photointermediates with absorption bands ranging from the red to the violet regions of the optical spectrum. During these photochemical transformations, bR pumps a proton from one side of the PM to the other side (Birge, 1990; Oesterhelt, 1998; Lanyi, 2006), which leads to a change in the local pH in the vicinity of the membrane and generation of an electrical response from an oriented PM in the presence of electrodes (Robertson and Lukashev, 1995; Chu et al., 2010). Due to these unique properties, bR is considered to be a promising material for bioelectronics and optoelectronics (Oesterhelt et al., 1991; Bräuchle et al., 1991; Hampp, 2000; Li et al., 2018), in particular, for designing photovoltaic cells (Xu et al., 2003; Chu et al., 2010; Renugopalakrishnan et al., 2014; Mohammadpour and Janfaza, 2015; Lu et al., 2016; Mohammadpour et al., 2016), optical memory elements (Hampp, 2000; Hillebrecht et al., 2005; Hudgins et al., 2010; Greco et al., 2012b; Ashwini et al., 2017), and holographic associative processors (Greco et al., 2012a), as well as for hydrogen production (Allam et al., 2011; Balasubramanian et al., 2013; Wang et al., 2014). Moreover, in comparison with chlorophyll, another biological component often used in designing hybrid optoelectronic systems, bR has a much simpler and more stable structure and can operate under intense radiation in the presence of oxygen for years, maintaining its efficiency at temperatures as high as 140 °C in the dry form and 80 °C in water at extreme pH values varying from 0 to

* Corresponding author.
** Corresponding author. Laboratoire de Recherche en Nanosciences, LRN-EA4682, Universite de Reims Champagne-Ardenne, 51100 Reims, France.
E-mail addresses: vkrivenkov@list.ru (V. Krivenkov), igor.nabiev@univ-reims.fr (I. Nabiev).

https://doi.org/10.1016/j.bios.2019.05.009
Received 5 March 2019; Received in revised form 14 April 2019; Accepted 3 May 2019
Available online 06 May 2019
0956-5663/

12.2 (Hampp, 2000).

However, a serious disadvantage of bR is that it has a very small absorption cross-section beyond its main absorption band, centered at 568 nm, with a full width at half maximum (FWHM) of ~100 nm (Stoeckenius et al., 1979). This disadvantage can be overcome by integrating additional "nano-antennas" into the bR-containing PMs in order to effectively absorb light energy in the spectral regions beyond the main bR absorption band and transfer it to bR. Semiconductor quantum dots (QDs) with very high extinction coefficients in the spectral range from UV to visible regions and photoluminescence (PL) quantum yields (QYs) reaching 100% have proved to be excellent "nano-antennas" for improvement of the bR biological function (Rakovich et al., 2010; Nabiev et al., 2010). Due to the easily controllable PL spectral position, QDs can efficiently transmit energy to bR by means of Förster resonance energy transfer (FRET) (Rakovich et al., 2010, 2014; Bouchonville et al., 2011, 2013; Oleinikov et al., 2012).

The photovoltaic properties of bR-containing PMs under one-photon excitation were demonstrated and employed in many applications (Robertson and Lukashev, 1995; He at al. 1998; Saga et al., 1999; Xu et al., 2003; Yen et al., 2010; Griep et al., 2010; Patil et al., 2012). Among many other studies, a solution-based photoelectrochemical cell designed by the group headed by El-Sayed has been described (Chu et al., 2010) and demonstrated the efficient photoelectrical signals without external bias. The studies of our and other groups cited above have demonstrated the possibility to employ QDs as build-in "nano-antennas" for efficient harvesting of visible light and its transfer to bR through FRET, thus enhancing its biological function (Griep et al., 2010; Rakovich et al., 2010; Bouchonville et al., 2011, 2013; Krivenkov et al. 2015, 2017).

It is worth mentioning that two-photon activation of the bR proton transfer function in the NIR region of the optical spectrum may be of particular interest for optoelectronic applications (Hampp, 2000), although the two-photon absorption cross-section of bR is as small as 290 GM (Birge et al., 1990). In contrast, QDs have uniquely large two-photon absorption cross-sections, reaching 50,000 GM (Hafian et al., 2014). Therefore, QD-based "nano-antennas" correctly incorporated in PMs should be able to absorb energy upon two-photon excitation in the NIR region and efficiently transfer the up-converted energy of two photons to bR through FRET, as shown in our previous study (Krivenkov et al., 2015).

The current methods for engineering bR-based photovoltaic cells operating in the NIR region of the optical spectrum employ up-conversion nanoparticles (UCNPs). UCNPs absorb light energy in the IR range of the optical spectrum and can reemit it in the visible range, where bR can effectively absorb light radiation (Lu et al., 2015, 2016). However, the existing UCNPs are nanocrystals doped with rare-earth elements (Wang et al., 2011) characterized by very low QYs (Boyer and Van Veggel, 2010) and discrete two-photon absorption spectra, covering limited wavelength ranges. The two-photon absorption spectra of QDs are continuous and cover wider wavelength ranges than those of UCNPs (Larson et al., 2003), thus providing obvious comparative advantages.

The present study is the first to demonstrate strong QD-mediated enhancement of the PM photoelectrical response under two-photon excitation. Moreover, we have demonstrated experimentally a 4.3-fold (+330%) increase in the light-to-electricity conversion efficiency of PM due to the FRET from QDs excited in the NIR region of the optical spectrum to bR in its native PMs. For this purpose, we engineered a bioinspired photoelectrochemical cell operating in the NIR region of the optical spectrum and employed the bR-containing PMs of *H. salinarum* with incorporated QDs as FRET "nano-antennas". The efficient excitation of QDs by two NIR photons followed by the one-photon transfer of energy absorbed and up-converted by QDs to the photosensitive retinal moiety of bR via FRET leads to a significant increase in the light energy conversion efficiency of the PMs. This is possible because QDs absorb the NIR light in the two-photon mode more efficiently than bR in PMs and then efficiently transfer this energy to the bR in PMs via FRET. The engineered QD–PM hybrid material can serve as a prototype component of novel bioinspired optoelectronic elements operating under two-photon excitation in the NIR spectral region.

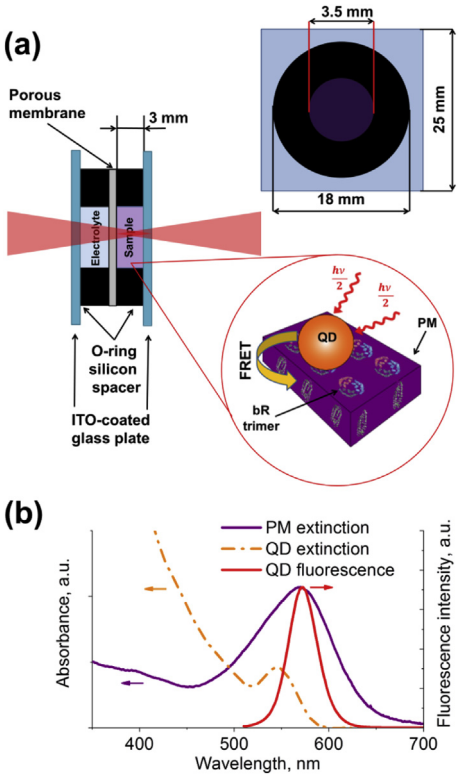

Fig. 1. Schematic structure of the photoelectrochemical cell and optical properties of the quantum dot (QD)–purple membrane (PM) complex. (a) Schematic representation of the QD–PM photoelectrochemical cell. (b) PM (purple solid line) and QD (orange dash–dot line) extinction spectra and QD fluorescence spectrum under two-photon excitation at 810 nm (red solid line). The figure shows only relative spectra positions and shapes. The absolute values of absorption coefficients and fluorescence intensities are not given. Colored arrows help to find the respective y-axis for spectrum with the same color. (For interpretation of the references to color in this figure legend, the reader is referred to the Web version of this article.)

2. Materials and methods

2.1. Experimental setup

The design of the photoelectrochemical cell employing QD–PM complexes was adapted from that proposed by El-Sayed and coworkers (Chu et al., 2010), where only PMs were used (Fig. 1a). The cell was fabricated from two identical half-cells separated by a porous dialysis membrane (MWCO, 12 kDa; Sigma-Aldrich). Each half-cell consisted of a 25 × 25 × 1.1 mm unpolished float glass plate passivated with a 200- to 300 Å layer of SiO_2 and coated on one side with a transparent indium tin oxide (ITO) layer with a surface resistance of 30–60 Ω/sq. On the ITO-coated side, a 3-mm-thick silicone ring with an inner diameter of 3.5 mm and an outer diameter of 18 mm was placed. The cavity inside the ring had a volume of ~30 µl. This cavity was filled with a QD, PM, or QD–PM solution in one of the two half-cells and with an electrolyte (borate buffer, pH 8) solution in the other half-cell. For two-photon excitation of this cell, we use pulsed laser radiation with a pulse duration of 80 fs, repetition rate of 80 MHz, and pulse energy ranging from 2.5 to 13.75 nJ (Tsunami, Spectra Physics), which was periodically switched on for 4.37 ms every 70 ms. The diameter of the excitation spot was ~50 µm. The experimental setup is described in detail

in the “Experimental setup” section of the Supporting Materials.

2.2. Material preparation

The *H. salinarum* PM sheets containing bR were prepared as described earlier (Rakovich et al., 2010). They had characteristic sizes from 50 to 1000 nm and the absorption spectra shown in Fig. 1b. White membranes (WMs) were prepared from PMs by means of bleaching of the retinal molecule (the only photosensitive fragment of bR) as described in (Birnbaum and Seltzer, 1992; Rakovich et al., 2010). The protocol of QD synthesis is provided in the Supporting Materials. QDs with a CdSe core and ZnS/CdS/ZnS multilayer shell where used because of their relatively small average diameter of ~5 ± 0.5 nm (Fig. S2 in the Supporting Materials) and high PL QY, which was found to be 90 ± 5% (in hexane), as measured by comparing the fluorescence of QDs and a reference fluorophore with a known QY (Rhodamine 6G). The two-photon absorption cross-section of QDs at 810 nm was measured by comparing the two-photon activated fluorescence of QDs and the reference fluorophore (Rhodamine 6G) with a known two-photon absorption cross-section of 70 GM (± 15%) (Makarov et al., 2008). It was found to be 16,000 GM (± 30%), as reported previously (Linkov et al., 2016). The method for calculation of the two-photon absorption cross-section is described in detail in the Supporting Materials. After the synthesis, the QDs were solubilized in aqueous borate buffer (pH 8) by coating them with an SH-[polyethylene glycol]-COOH (SH-PEG-COOH) organic shell using the ligand exchange technique (Sukhanova et al., 2012). This organic shell provides the QDs with a negative surface charge, which is necessary for efficient electrostatic interaction of the QDs with the positively charged amino acid groups on the surface of the PM, leading to formation of tight QD–PM complexes (Krivenkov et al., 2017). Borate buffer (pH 8) used as a solvent for all samples ensures a high photovoltaic performance of bR (Kuo and Chu, 2014; Robertson and Lukashev, 1995), as well as effective QD–bR complexation (Krivenkov et al., 2017). In order to guarantee highly efficient FRET from QDs to bR, we tuned the optical properties of QDs to maximize the overlap integral (eq. S(5) in the Supporting Materials) between the bR absorption and the QD PL bands (Fig. 1), which finally reached 6.1×10^{-13} cm^3/M. The measured QY of QDs in the borate buffer solution was 50%; thus, the calculated FRET distance for the QD–bR pair was 6.1 nm. The hydrodynamic diameter of water-solubilized QDs was measured by the dynamic light scattering technique using a Malvern Zeta Sizer Nano ZS. Its mean value was found to be ~7 nm.

3. Results and discussion

3.1. Fabrication of the quantum dot–purple membrane hybrid material

The first goal of this study was the fabrication of the QD–PM hybrid material, the active media of the photoelectrochemical cell, with its efficient operation ensured by selection of the concentrations of bR and QDs and the conditions for their complexation. To determine the molar concentration of bR required for efficient operation of the designed photoelectrochemical cell, we have measured the photoelectric signals of a cell containing only PMs as the active media under two-photon excitation. The experiments were carried out at bR molar concentrations varying from 0.33×10^{-5} to 5×10^{-5} M (Fig. 2a) and average laser powers of 400, 600, 800, and 1000 W (Fig. 2b). To evaluate the efficiency of the photoelectrochemical cell, we measured the energy E released in the circuit during one laser excitation period T. The excitation period was calculated using the measured signals $I(t)$ at the whole resistance value R calculated to be ~100 Ω:

$$E \sim \int_0^T I^2(t) R dt. \quad (1)$$

As one can see from Fig. 2c, the photoelectric energy generated by the photoelectrochemical cell increases linearly (R^2 from 0.995 to 0.999) with increasing bR molar concentration up to 3.3×10^{-5} M and reaches saturation at a concentration of 5×10^{-5} M, which is most clearly visible at high intensities of excitation. This saturation can be explained by direct dependence of the photoelectrical signal on the amount of PMs adsorbed on the electrode surface, which, in turn, follows the Langmuir law (Hanaor et al., 2014), gradually approaching saturation.

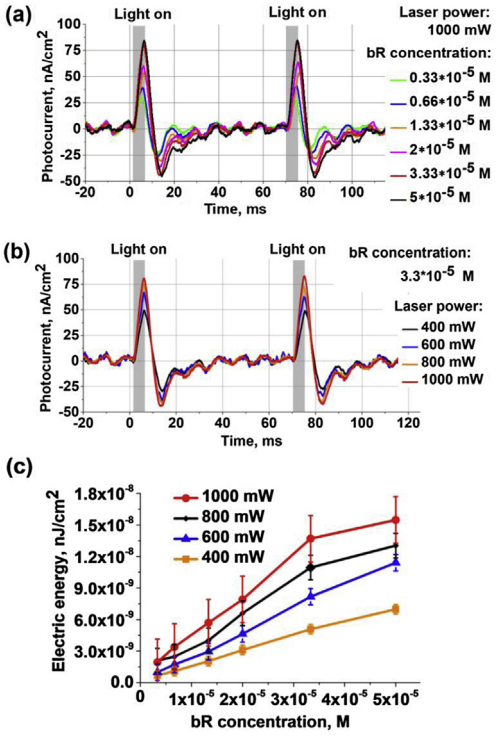

Fig. 2. Photoelectrical response from a photoelectrochemical cell filled with purple membranes as an active material. (a) Photoelectric signals at an excitation power of 1000 mW at different bacteriorhodopsin (bR) concentrations. (b) Photoelectric signals upon laser excitation at different powers and a bR molar concentration of 3.3×10^{-5} M. (c) The dependences of the photoelectrical energy released by the photoelectrochemical cell during one excitation period on the concentration of bR at different laser excitation powers. From 3 to 5 measurements were performed to calculate the average value and error for each experimental point in the graphs in Fig. 2c. (For interpretation of the references to color in this figure legend, the reader is referred to the Web version of this article.)

The next goal was to determine which bR-to-QD molar ratio will provide the most efficient increase in light-to-electricity conversion. Previously we have found that an increase in the bR-to-QD molar ratio leads to an increased number of QD–PM complexes and efficiency of the energy transfer (Krivenkov et al., 2015). However, the bR molecules in PMs are organized in the form of trimers located at distances of about 6.2 nm from one another (Butt et al., 1990; Rakovich et al., 2010; Bouchonville et al., 2011). This means that a QD with a hydrodynamic diameter of 7 nm deposited on the surface of the PM will never interact with a single bR molecule, but will instead spread the energy transferred by FRET over the whole bR trimer. The bR-to-QD molar ratio of 3:1 corresponds to the interaction of a single QD with three bR molecules forming a trimer. Thus, upon an increase in the bR concentration beyond that corresponding to a bR-to-QD ratio of 3:1, many bR molecules will not interact with QDs, and efficient FRET from QDs to these bR molecules under two-photon excitation will not be possible. The efficiency of FRET in the QD–PM material was determined as the efficiency of quenching the donor (QD) luminescence in the presence of the acceptor (retinal of bR). In our experiment, the luminescence

quenching efficiency for the bR-to-QD molar ratio of 3:1 was found to be 40% (Fig. S3 in the Supporting Materials).

To prove that this quenching is due to FRET rather than other quenching mechanisms, we obtained complexes of QDs with WMs, from which retinal, the photosensitive component of bR, had been extracted and where FRET was impossible because of the absence of the acceptor (Rakovich et al., 2010). In our experiment, the WMs concentration equal to the PM concentration in the QD–PM material was used. Although the WM surface was equal to that of PMs, the PL quenching in the QD–WM material was found to be only 10% (Fig. S3 in the Supporting Materials). Thus, the luminescence quenching accounted by FRET was 30%. Although the average FRET efficiency in a solution increases with an increase in the bR-to-QD molar ratio (Krivenkov et al., 2017), our experimental results show that the 10% increase in FRET efficiency requires a 333% increase in the bR-to-QD molar ratio from 3:1 to 10:1 (Fig. S3 in the Supporting Materials). In this case, 70% of bR molecules will not effectively interact with QDs (Bouchonville et al., 2013).

According to the above experimental results and considerations, we have prepared a hybrid material in the form of QD–PM complexes with a bR concentration of 3.3×10^{-5} M and a QD concentration of 1.1×10^{-5} M (a bR-to-QD molar ratio of 3:1) to be used as an active medium in the photoelectrochemical cell. Considering that the calculated Förster distance (Eq. S(4) in Supporting Materials) for the QD–bR pair was 6.1 nm and the measured FRET efficiency was 30%, the average distance between QD and bR in the solution was calculated to be 8.6 nm (Eq. S(3) from Supporting Materials). This distance is quite realistic for tight QD–PM complexes (Bouchonville et al., 2013), because the radius of QDs is about 3.5 nm and the retinal acceptor depth in PM is about half the thickness of the PM (up to 3 nm). The method of calculating the Förster distance and FRET efficiency is described in detail in the section "Förster resonance energy transfer (FRET) efficiency analysis" of the Supporting Materials.

3.2. The effect of quantum dots on the efficiency of light-to-electricity energy conversion in the quantum dot–purple membrane hybrid material

The main goal of our study was to determine the effect of QDs on the photoelectric signals from PMs. For this purpose, we have measured the photoelectric signals from a cell containing PMs or QDs alone, or the QD–PM hybrid material (Fig. 3 and Fig. S4 in the Supporting Materials). For comparison, Fig. 3a also shows the photoelectric signals from the pure electrolyte as a ground signal, from pure PMs without QDs, and from pure QDs without PMs at an excitation laser power of 1100 mW. One can see from Fig. 3a that the signal from QD–PM hybrid complexes is much higher than the superposition of the signals from pure QDs and pure PMs (the positive branch is increased by a factor of 2.3 ± 0.2, and the negative one, by a factor of 1.9 ± 0.2). This confirms that the QDs in the photoelectrochemical cell transfer additional energy to bR under two-photon excitation, thus improving the photoelectric properties of PMs. The weak photoelectric signal from pure QDs without PMs is probably due to the photoinduced release of charges from the QDs, which can be observed in the solutions (Krivenkov et al., 2018) instead of fluorescence intermittency (blinking). To evaluate experimentally the effect of QDs on the efficiency of light-to-electricity conversion by PMs under two-photon excitation, we measured the dependence of the energy of the electric signal (Eq. (1)) on the laser excitation power for QD–PM complexes and compared it with this dependence for PMs and QDs alone (Fig. 3b). One can see that the complexation of QDs and PMs lead to a strong enhancement of the energy of electric signal for a wide range of excitation intensities, from 50 to 1100 mW. Fig. 3c shows the ratios of the signal energy from the QD–PM material to the signal energy from pure PMs as a function of the power of excitation. The data show that the conversion efficiency was enhanced, on average, by a factor of 4.3 ± 0.6, whereas under one-photon excitation of the same complexes, this effect is 3–4 times smaller (Griep et al., 2010).

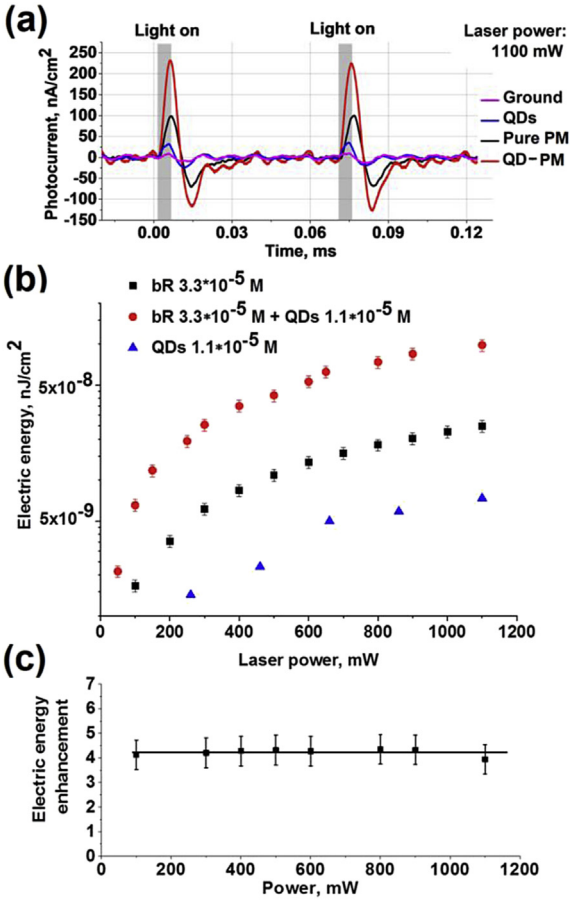

Fig. 3. Comparison of the photoelectrical signals from the photoelectrochemical cell filled with quantum dot (QD)–purple membrane (PM) complexes, pure PMs, and pure QDs. (a) Photoelectric signals from the photoelectrochemical cell filled with PMs (black line), QDs (blue line), and QD–PM complexes (red line) under two-photon excitation at 1100 mW. (b) Dependences of the energy of the photoelectrical signal from the photoelectrochemical cell on the power of two-photon excitation for PMs (black squares), QDs (blue triangles), and QD–PM complexes (red circles) used as active media. (c) Enhancement factor of the energy of the photoelectrical signal from the photoelectrochemical cell filled with QD–PM as compared to pure PMs at different laser excitation powers. From 3 to 5 measurements were performed to calculate the average value and error for each experimental point in the graphs in Fig. 2b and c. (For interpretation of the references to color in this figure legend, the reader is referred to the Web version of this article.)

We found the value of this increase quite reasonable due to the following reasons. The two-photon absorption cross-section of bR at the wavelength of 810 nm was found to be about 200 GM (Birge et al., 1990), whereas the two-photon absorption cross-section of the QDs used in this study was measured to be about 16,000 GM (± 30%), about 80 times larger than that of bR. This means that, at the same excitation conditions, a single QD can absorb 80 times more energy than a single bR molecule. The bR-to-QD molar ratio in this study was about 3, and the efficiency of the energy transfer from QDs to bR was about 30%. This means that a QD can transfer 10% of the absorbed energy to each bR molecule, and this amount of energy is 8 times higher than the energy absorbed by each bR itself. Therefore, the efficiency of light-to-electricity conversion by PMs may be expected to increase by a factor as high as 8. However, this value can be considered to be only an order-of-magnitude approximation for the values observed for the experimental QD–PM complex, rather than an exact estimate. It should be mentioned that direct excitation of bR in the two-photon absorption mode takes place in the transition region with energies of about 3.1 eV, whereas its excitation via FRET from the QDs is essentially one-photon

process, and the corresponding transition is in the region of the maximum fluorescence of QDs, at energies of about 2.2 eV. Thus, these two modes of bR excitation differ not only in the energies of the absorption transitions, but also in the selection rules, which are generally different for one-photon and two-photon transitions. This makes it difficult to obtain an accurate theoretical estimate of the possible increase in the photoelectrical signal in such a complex system. This is why the main result of our study is the careful experimental determination of the QD-induced increase in the PM photoelectrical response in the designed photoelectrochemical cell.

The results confirm our assumption that the QD "nano-antennas" can significantly (by 330%) enhance the efficiency of light energy conversion by bR under two-photon excitation. The main cause of the enhancement is that QDs absorb NIR light more efficiently than PMs and transfer it to the PMs via FRET. Doing so, QDs work as light energy concentrators in QD-PM complexes transferring the additional energy to PMs, thus enhancing the PM light-to-electricity conversion efficiency. An even greater enhancement should be possible upon an increase in the efficiency of the formation of QD–PM complexes, when all QDs and all bR trimers will be coupled at the minimal distances from each other while maintaining the high efficiency of FRET within each complex. This task, however, can be quite complicated, because such a specific chemical binding should be obtained with very short molecules, providing a small distance (of the order of the Förster distance R_0 = 6.1 nm) between the centers of the QDs and the center of the PM, which corresponds to a distance between their surfaces of about 1–2 nm (Bouchonville et al., 2013). An alternative method is the use of nanocrystals with a larger two-photon absorption cross-section (for example, nanorods), which, however, leads to an increase in the size of the "donor" nanocrystal, and, hence, in the donor–acceptor distance.

4. Conclusions

This study has directly demonstrated the possibility of initiation of a bR photocycle through FRET from QDs to bR under two-photon excitation in the NIR region of the optical spectrum. The possibility of using two-photon excitation of QD–PM complexes to convert light into electrical energy has also been demonstrated in this study for the first time. The data show that QD-induced increase in the efficiency of light-to-electricity conversion in QD–PM complexes compared with pure PMs was as high as 330% (by a factor of 4.3). The observed increase has been explained by our previously proposed hypothesis that QDs in the fabricated QD–PM material act as built-in "nano-antennas" effectively harvesting NIR light and then transmitting the absorbed and up-converted energy to bR by means of FRET.

To obtain these experimental results, we have engineered a photoelectrochemical cell operating under nonlinear two-photon excitation in the NIR spectral region and fabricated a hybrid material in the form of an aqueous solution of electrostatically bound complexes of PMs and CdSe/ZnS/CdS/ZnS QDs coated with an SH-PEG-COOH organic shell. Then, we have selected the hybrid material composition that is optimal for efficient cell operation and measured the FRET efficiency in this material. We have measured the electrical signals from the cells containing pure PMs, pure QDs, or QD–PM hybrid material and shown that the use of the QD–PM material instead of pure PMs enhances the efficiency of light-to-electrical conversion by a factor of 4.3 under two-photon excitation. The nature of the enhancement of the conversion efficiency of PMs in the hybrid complexes with QDs is in the high two-photon absorption cross-section of QDs. This means that QDs absorb light in the two-photon mode more efficiently than PMs and not only utilize this energy themselves, but transfer it to the PMs via FRET. Thus, QDs work as light energy concentrators transferring the additional energy to PMs, thereby increasing the conversion efficiency of the PMs.

Because efficient two-photon excitation of the QD–bR material requires intense laser irradiation, the discovered effect cannot be employed in photovoltaics. However, the nonlinear nature of two-photon excitation provides considerable comparative advantages, such as a sharp threshold of radiation sensitivity and the possibility of precise three-dimensional location of objects in holographic and optical computing. Moreover, this concept may have applications in the field of biosensing in the following manner. A change in the distance between a QD and bR due to the adsorption of the detected objects will lead to a change in the efficiency of FRET and a sharp drop of the photoelectric signal from the cell. In addition, two-photon excitation of QDs can be implemented in the NIR spectral "transparency window" of biological tissues. Therefore, this method could provide a high sensitivity and contrast. Thus, the results of this study may extend the use of bioinspired hybrid materials in optoelectronics, holography, bioelectronics, and biosensing.

CRediT authorship contribution statement

Victor Krivenkov: Investigation, Methodology, Writing - original draft. **Pavel Samokhvalov:** Investigation, Methodology, Writing - review & editing. **Igor Nabiev:** Conceptualization, Resources, Supervision, Writing - review & editing.

Acknowledgements

This study was supported by the Russian Science Foundation, grant no. 18-72-10143. We thank Vladimir Ushakov for the help with technical preparation of the manuscript.

Appendix A. Supplementary data

Supplementary data to this article can be found online at https://doi.org/10.1016/j.bios.2019.05.009.

References

Allam, N.K., et al., 2011. Energy Environ. Sci. 4, 2909. https://doi.org/10.1039/c1ee01447a.
Ashwini, R., et al., 2017. Curr. Microbiol. 74, 996–1002. https://doi.org/10.1007/s00284-017-1271-5.
Balasubramanian, S., et al., 2013. Nano Lett. 13, 3365–3371. https://doi.org/10.1021/nl4016655.
Birge, R.R., 1990. Biochim. Biophys. Acta Bioenerg. 1016, 293–327. https://doi.org/10.1016/0005-2728(90)90163-X.
Birge, R.R., et al., 1990. Mol. Cryst. Liq. Cryst. Inc. Nonlinear Opt. 189, 107–122. https://doi.org/10.1080/00268949008037226.
Birnbaum, D., Seltzer, S., 1992. Photochem. Photobiol. 55, 745–752. https://doi.org/10.1111/j.1751-1097.1992.tb08520.x.
Bouchonville, N., et al., 2013. Laser Phys. Lett. 10 085901. https://doi.org/10.1088/1612-2011/10/8/085901.
Bouchonville, N., et al., 2011. Appl. Phys. Lett. 98 013703. https://doi.org/10.1063/1.3533392.
Boyer, J.-C., Van Veggel, F.C.J.M., 2010. Nanoscale 2, 1417–1419. https://doi.org/10.1039/c0nr00253d.
Bräuchle, C., et al., 1991. Adv. Mater. 3, 420–428. https://doi.org/10.1002/adma.19910030903.
Butt, H.J., et al., 1990. Biophys. J. 58, 1473–1480. https://doi.org/10.1016/S0006-3495(90)82492-9.
Chu, L.-K., et al., 2010. Biosens. Bioelectron. 26, 620–626. https://doi.org/10.1016/j.bios.2010.07.013.
Greco, J.A., et al., 2012a. Int. J. Unconv. Comput. 8, 433–457.
Greco, J.A., et al., 2012b. Biomolecular electronics and protein-based optical computing. In: Katz, E. (Ed.), Biomolecular Information Processing. Wiley-VCH Verlag GmbH & Co. KGaA, Weinheim, Germany, pp. 33–59. Biomolecular Information Processing: From Logic Systems to Smart Sensors and Actuators. https://doi.org/10.1002/9783527645480.ch3.
Griep, M.H., et al., 2010. Biosens. Bioelectron. 25, 1493–1497. https://doi.org/10.1016/J.BIOS.2009.11.005.
Hafian, H., et al., 2014. Nanomedicine 10, 1701–1709. https://doi.org/10.1016/j.nano.2014.05.014.
Hampp, N., 2000. Chem. Rev. 100, 1755–1776.
Hanaor, D.A.H., et al., 2014. Langmuir 30, 15143–15152. https://doi.org/10.1021/la503581e.
He, J.-A., et al., 1998. J. Phys. Chem. B 102, 7067–7072. https://doi.org/10.1021/jp981612x.
Hillebrecht, J.R., et al., 2005. NanoBiotechnology 1, 141–152. https://doi.org/10.1385/NBT:1:2:141.

Hudgins, M., et al., 2010. J. Nanoelectron. Optoelectron. 5, 287–289. https://doi.org/10.1166/jno.2010.1111.
Krivenkov, V., et al., 2015. Opt. Lett. 40, 1440–1443. https://doi.org/10.1364/OL.40.001440.
Krivenkov, V.A., et al., 2017. Optic Spectrosc. 122, 42–47. https://doi.org/10.1134/S0030400X1701012X.
Krivenkov, V., et al., 2018. J. Phys. Chem. C acs.jpcc.8b04544. https://doi.org/10.1021/acs.jpcc.8b04544.
Kuo, C.-L., Chu, L.-K., 2014. Bioelectrochemistry 99, 1–7. https://doi.org/10.1016/J.BIOELECHEM.2014.05.003.
Lanyi, J.K., 2006. Biochim. Biophys. Acta Bioenerg. 1757, 1012–1018. https://doi.org/10.1016/j.bbabio.2005.11.003.
Larson, D.R., et al., 2003. Science 300, 1434–1436. https://doi.org/10.1126/science.1083780.
Li, Y.-T., et al., 2018. Sensors 18, 1368. https://doi.org/10.3390/s18051368.
Linkov, P., et al., 2016. Mater. Today Proc. 3, 104–108.
Lu, Z., et al., 2016. Nanoscale 8, 18524–18530. https://doi.org/10.1039/C6NR06930D.
Lu, Z., et al., 2015. Chem. Commun. 51, 6373–6376. https://doi.org/10.1039/C5CC00457H.
Makarov, N.S., et al., 2008. Opt. Express 16, 4029–4047. https://doi.org/10.1364/OE.16.004029.
Mohammadpour, R., Janfaza, S., 2015. ACS Sustain. Chem. Eng. 3, 809–813. https://doi.org/10.1021/sc500617w.
Mohammadpour, R., et al., 2016. Biomass Bioenergy 87, 35–38. https://doi.org/10.1016/J.BIOMBIOE.2015.10.017.
Nabiev, I., et al., 2010. Angew Chem. Int. Ed. Engl. 49, 7217–7221. https://doi.org/10.1002/anie.201003067.
Oesterhelt, D., 1998. Curr. Opin. Struct. Biol. 8, 489–500. https://doi.org/10.1016/S0959-440X(98)80128-0.
Oesterhelt, D., et al., 1991. Q. Rev. Biophys. 24, 425. https://doi.org/10.1017/S0033583500003863.
Oesterhelt, D., Stoeckenius, W., 1971. Nature 233, 149. https://doi.org/10.1038/10.1038/newbio233149a0.
Oleinikov, V., et al., 2012. SPIE Proc 8464, 84640Z. https://doi.org/10.1117/12.929764.
Patil, V.A., et al., 2012. J. Phys. Chem. B 116, 683–689. https://doi.org/10.1016/10.1021/jp210520k.
Rakovich, A., et al., 2014. J. Photochem. Photobiol. C Photochem. Rev. 20, 17–32. https://doi.org/10.1016/j.jphotochemrev.2014.04.001.
Rakovich, A., et al., 2010. Nano Lett. 10, 2640–2648. https://doi.org/10.1021/nl1013772.
Renugopalakrishnan, V., et al., 2014. J. Phys. Chem. C 118, 16710–16717. https://doi.org/10.1021/jp502885s.
Robertson, B., Lukashev, E.P., 1995. Biophys. J. 68, 1507–1517. https://doi.org/10.1016/S0006-3495(95)80323-1.
Saga, Y., et al., 1999. J. Phys. Chem. B 103, 234–238. https://doi.org/10.1021/jp982144u.
Stoeckenius, W., et al., 1979. Biochim. Biophys. Acta Rev. Bioenerg. 505, 215–278. https://doi.org/10.1016/0304-4173(79)90006-5.
Sukhanova, A., et al., 2012. Nanomed. Nanotechnol. Biol. Med. 8, 516–525. https://doi.org/10.1016/j.nano.2011.07.007.
Wang, H.-Q., et al., 2011. Adv. Mater. 23, 2675–2680. https://doi.org/10.1002/adma.201100511.
Wang, P., et al., 2014. ACS Nano 8, 7995–8002. https://doi.org/10.1021/nn502011p.
Xu, J., et al., 2003. Biophys. J. 85, 1128–1134. https://doi.org/10.1016/S0006-3495(03)74549-4.
Yen, C.-W., et al., 2010. J. Am. Chem. Soc. 132, 7250–7251. https://doi.org/10.1021/ja101301u.